Synthesis and Characterization of Nanosized α-LiFeO$_2$ with Increased Electrochemical Activity

Yourong Wang[*], Jia Wang, Hantao Liao, Xiaofang qian, Yuchan Zhu[*], Siqing Cheng

Chemical and Environmental Engineering Department, Wuhan Polytechnic University, Wuhan 430023, Hubei, P.R.China
[*]E-mail: wyourong@163.com; zhuyuchan@163.com

In this work, nanosized α-LiFeO$_2$ were synthesized by a simple low-temperature solid state method. The obtained α-LiFeO$_2$ nanoparticles were investigated by the measurements of X-ray diffraction pattern, scanning electronic microscopy, transmission electron microscope and electrochemical performance. Electrochemical measurements showed that the initial discharge capacity was 277.9, 188.4, and 158.2 mAh g^{-1} at 0.1 C, 1 C, and 2 C, respectively. Meanwhile, the α-LiFeO$_2$ nanoparticles exhibited improved cycle stability (123 mAh g^{-1} at 2 C after 60 cycles). The high capacity, improved rate performance and cycle stability can be attributed to the smaller particle sizes, which can facilitate the contact between active materials and the electrolyte, enhance lithium and electron transport during cycling.

1. INTRODUCTION

Significant efforts have been devoted to maximize both their energy density and safety to produce an advanced energy storage system. Transition metal compounds are promising cathode materials for lithium secondary batteries [1–3]. Because of the low cost, environmentally benignity, better safety and the most abundant metal available in the world [4]. Iron-based compounds have attracted the attention of scientists for a long time, showing a big advantage compared to LiCoO$_2$ and LiNiO$_2$ for practical use [5]. As an important transition metal compound，Lithium ferrite (LiFeO$_2$) has attracted much attention as active materials for rechargeable Li batteries due to its high capacity. It is well known that LiFeO$_2$ has various crystalline structures, such as α-LiFeO$_2$ [6-8], goethite-type LiFeO$_2$ [9], hollandite-type LiFeO$_2$ [10], corrugated layer LiFeO$_2$ [11-14]. The crystalline structure of

$LiFeO_2$ depends mainly on the preparation route. For electro active $\alpha\text{-}LiFeO_2$ materials, various synthesis routes have been proposed: ion-exchange method, hydrothermal synthesis, solvent-thermal synthesis, low-temperature solid state reaction, low-temperature molten salt method. The $\alpha\text{-}LiFeO_2$ nanoparticles with the size of ~50 nm were prepared by solid state reaction at 250 ºC, which presented a capacity of 150 mAh g^{-1} at 0.25 C in the range of 4.5-1.5 V after 50 cycles [15]. Very recently, the $\alpha\text{-}LiFeO_2$ nanoparticles with the size of ~10 nm were prepared by one step molten salt route at 120 ºC, which showed initial capacities of 138 and 71 mAh g^{-1} at 1.0 and 2.0 C [16]. However, many problems still remain, such as poor rate performance and low capacity retention during cycling tests [17, 18]. So it is still a great challenge to improve both the cycling stability and the rate capability of $\alpha\text{-}LiFeO_2$ electrode materials. It is demonstrated that the capacity retention of electrode materials can be improved via fabricating active materials into nano-structures. The nano-structure materials could accommodate volume changes and shorten the lithium diffusion length [19-23], which are beneficial to improving the rate performance and cycle life of the materials for lithium ion batteries [24, 25]

Here, we report the synthesis of $\alpha\text{-}LiFeO_2$ nanoparticles by a conventional solid state method using very low temperature and without further heat treatment. And the electrochemical properties of the obtained $\alpha\text{-}LiFeO_2$ nanoparticles were investigated under different current density. The electrochemical measurements have demonstrated that the $\alpha\text{-}LiFeO_2$ nanoparticles can be used as a novel cathode material in lithium-ion batteries. Moreover, the obtained $\alpha\text{-}LiFeO_2$ nanoparticles show high capacity, good cycling stability, and high-rate capability compared to those previously reported results.

2. EXPERIMENTAL

All reagents were analytically pure from the commercial market and were used as received without further purification. The nanosized $\alpha\text{-}LiFeO_2$ material was prepared by a facile low-temperature solid state method: $LiOH \cdot H_2O$ (Changzhou Chenhua Chemicals, 95.0%), $LiNO_3$ (Tianjin Kemiou Chemical Reagent, 99.0 %) and $Fe(NO_3)_3 \cdot 9H_2O$ (Tianjin Baishi Chemicals, 98.5%) in the molar ratio (Li/Fe=20) were used as raw materials. The starting materials were thoroughly mixed and hand ground with a pestle, then the well-mixed powders were heated in a box furnace at set temperature for 3 h in air. Finally，the solid product was collected, washed repeatedly with distilled water, ethanol, and dried at 80℃ under vacuum.

The crystalline phase of the prepared $\alpha\text{-}LiFeO_2$ was identified by powder X-ray diffraction with a shimadzu XRD-6000 diffractometer using Cu Kα radiation (λ = 1.5418 Å) and a scanning step of 2° per minute. The morphology of the prepared $\alpha\text{-}LiFeO_2$ was observed by Scanning Electron Microscopy (SEM) with Hitachi FEG SEM and Transmission Electron Microscope (HRTEM, JEOL-2010) with an accelerating voltage of 200 kV.

The composite electrodes were prepared using the following procedure: 0.03 g of polyvinylidene difluoride (PVDF) was first added to *N*-Methyl pyrrolidone (NMP) to form the homogenous solution. Then, the prepared powders and acetylene black (the weight ratio of the prepared powders /acetylene black/ PVDF was 7:2:1) were added to the solution above. The obtained

mixture was dispersed by utilizing ultrasonic technology. Subsequently, the mixture was dropped to a piece of aluminum foil. Finally, the aluminum foil coated with the mixture was dried at 80℃ for 24 h. The composite electrodes were subsequently assembled into Coin-type 2016 cells using Metallic lithium as the anode with a micro-porous membrane separator (Celguard^R 2325,American) and liquid electrolyte mixtures containing 1 mol L^{-1} LiPF$_6$ and a solvent mixture of ethylene carbonate and dimethyl carbonate (1:1, v/v).The cells were assembled in a glove box filled with pure argon.

The electrochemical properties of α-LiFeO$_2$ nanomaterials were measured by a program-controlled Battery Test System (Land$^®$, Wuhan, China). The charge and discharge characteristics of α-LiFeO$_2$ nanomaterials were evaluated at various currents (0.1 C, 0.5 C, 1 C, 2 C rates) in the voltage range of 1.5–4.5 V vs. Li$^+$/Li at room temperature. The cyclic voltammetry (CV) was performed in a three-electrode cell with lithium foil as counter and reference electrodes by using a CHI660B Electrochemical Work-station (Chenghua, Shanghai, China) at room temperature. The CV tests were carried out at potential scan rate of 0.2 mV s^{-1}.
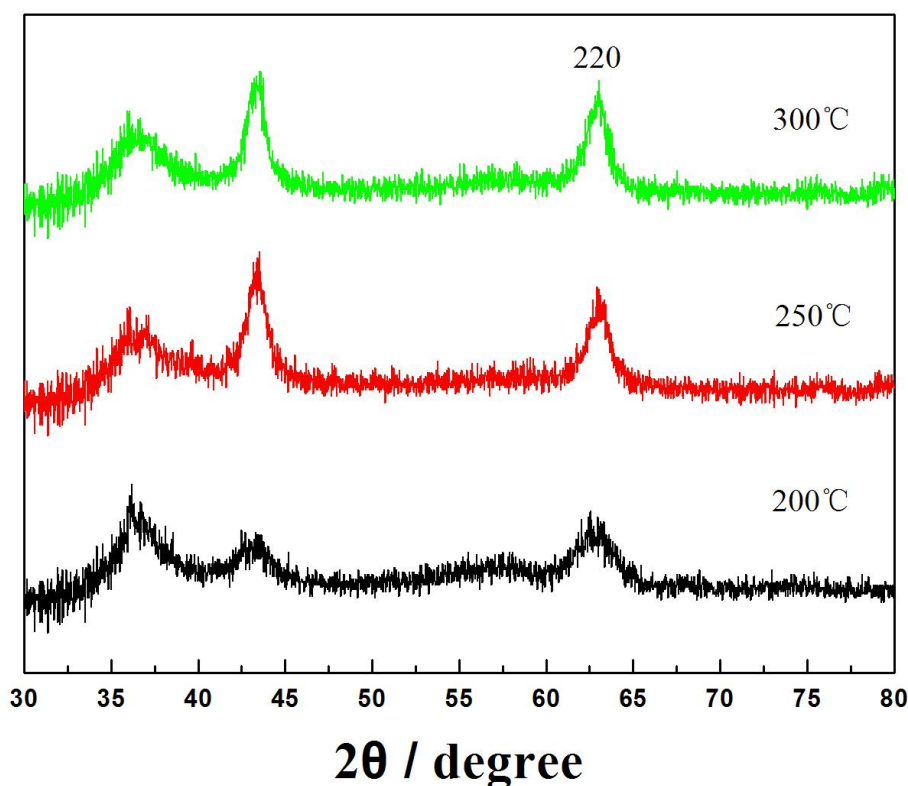
3. RESULTS AND DISCUSSION

Figure 1. XRD patterns of the obtained products

In the solid-state synthesis, the sintering temperature has considerable effect on the structure and crystallinity. Figure 1 shows the XRD pattern of the resulting products prepared by solid-state

reaction under the different synthetic temperatures. From Figure 1, it can be seen that all the diffraction peaks can be easily indexed to a pure cubic phase of α-LiFeO$_2$, which matches well with the reported value (JCPDS 74-2284). The XRD pattern indicates that pure α-LiFeO$_2$ can be obtained under current synthetic conditions. It is worthy of note that the sample prepared at 200℃ shows a decrease in the intensity of the main peaks, which clearly indicated that the crystallinity of the prepared samples decrease with temperature decreasing. The broadening of all the peaks indicates small particle size. The approximate crystallite sizes of the α-LiFeO$_2$ samples prepared at 250℃ were calculated using the Debye–Scherrer equation applied to the marked peaks (2 2 0), and the crystal sizes were 11.08nm.
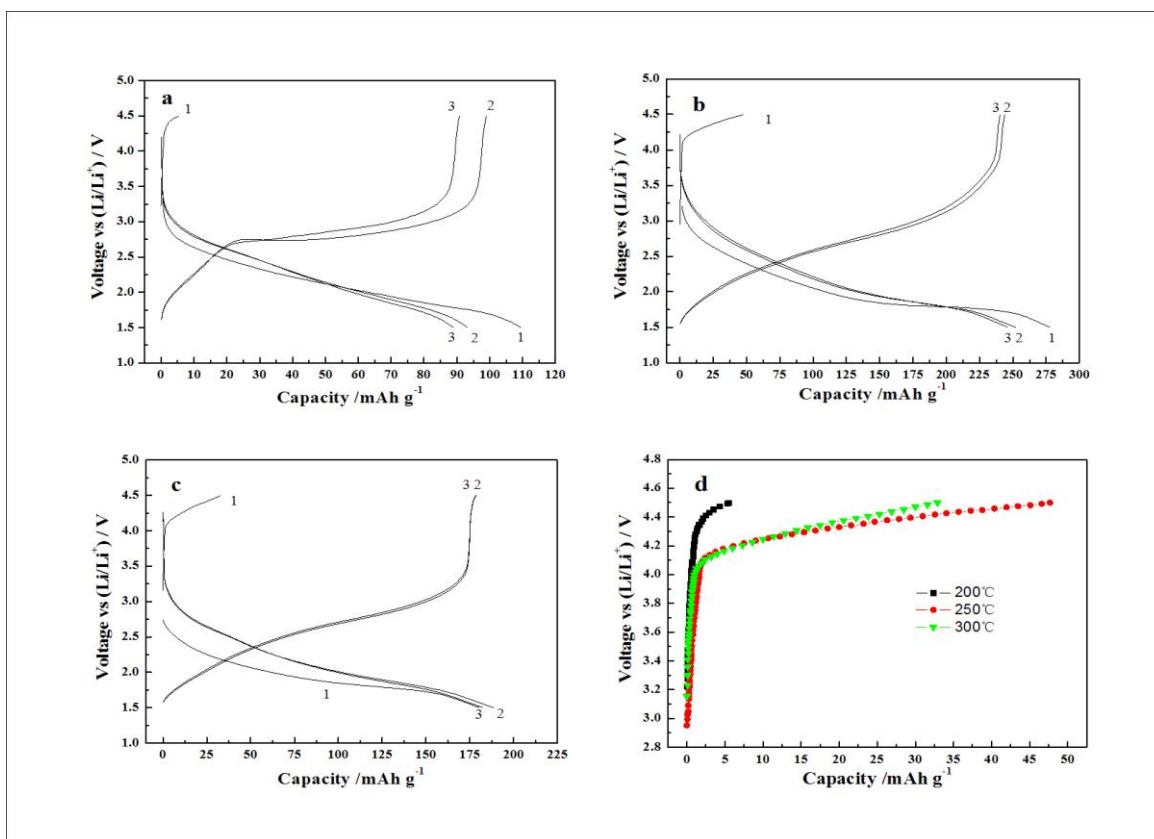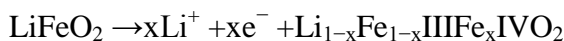

Figure 2. Charge–discharge curves for different cycles of α-LiFeO$_2$ electrodes prepared at different temperature. a 200℃, b 250℃, c 300℃ and charge curves for the first cycle at different temperature

In order to investigate the electrochemical properties of the α-LiFeO$_2$ electrodes prepared at different temperature, an electrochemical test is conducted for the α-LiFeO$_2$ electrodes at room temperature. Figure 2 depicts charge–discharge curves for different cycles of α-LiFeO$_2$ electrodes at 0.1 C between 1.5 and 4.5 V. From Figure 2a, 2b and 2c, it can be seen that the α-LiFeO$_2$ electrodes prepared at 200, 250 and 300 ∘C deliver a discharge capacity of 109.5, 277.9 and 180.6 mAh g^{-1} in the first cycle, respectively. The highest initial discharge capacity is obtained by the α-LiFeO$_2$ electrodes synthesized at 250∘C, which is higher than those reported for nano-LiFeO$_2$ [6, 26]. Meanwhile, it can be clearly seen that the curves in the first cycle are significantly different from those in the second and

third cycles for all the α-LiFeO$_2$ electrodes. On charging in the first cycle, the voltage exhibits an abrupt increase from 3.0 (OCV) to 4.0 V, subsequent a pseudo-plateau is observed. The phenomenon is clearly seen in Figure 2d. The reaction taking place in the electrode during the charge process is believed to be as follows:

$$LiFeO_2 \rightarrow xLi^+ + xe^- + Li_{1-x}Fe_{1-x}^{III}Fe_x^{IV}O_2$$

However, large voltage hysteresis is observed during the discharge step, the discharge voltage decreases rapidly to 3 V at the beginning, then, the slope changed and a pseudo-plateau that extending to ca. 1.7 V is observed. In contrast, the charge and discharge curves in the subsequent cycles differ from those in the first cycle. The pseudo-plateau above 4 V disappears in the subsequent charge process and S-shape curves are observed in the 3-V region, while the voltage of the discharge curve in the subsequent discharge process is higher. These results indicate that the electrochemical reaction of α-LiFeO$_2$ nanomaterials during the initial charge-discharge has a different mechanism from that of subsequent cycles. The reason is attributed to irreversible structure change during the first charge [27]. To better understand the irreversible cycle behavior during the first discharge process, a cyclic voltametry analysis was carried out at a sweep rate of 0.2 mV/s between the voltage limits of 1.5–4.5 V (Li/Li$^+$).
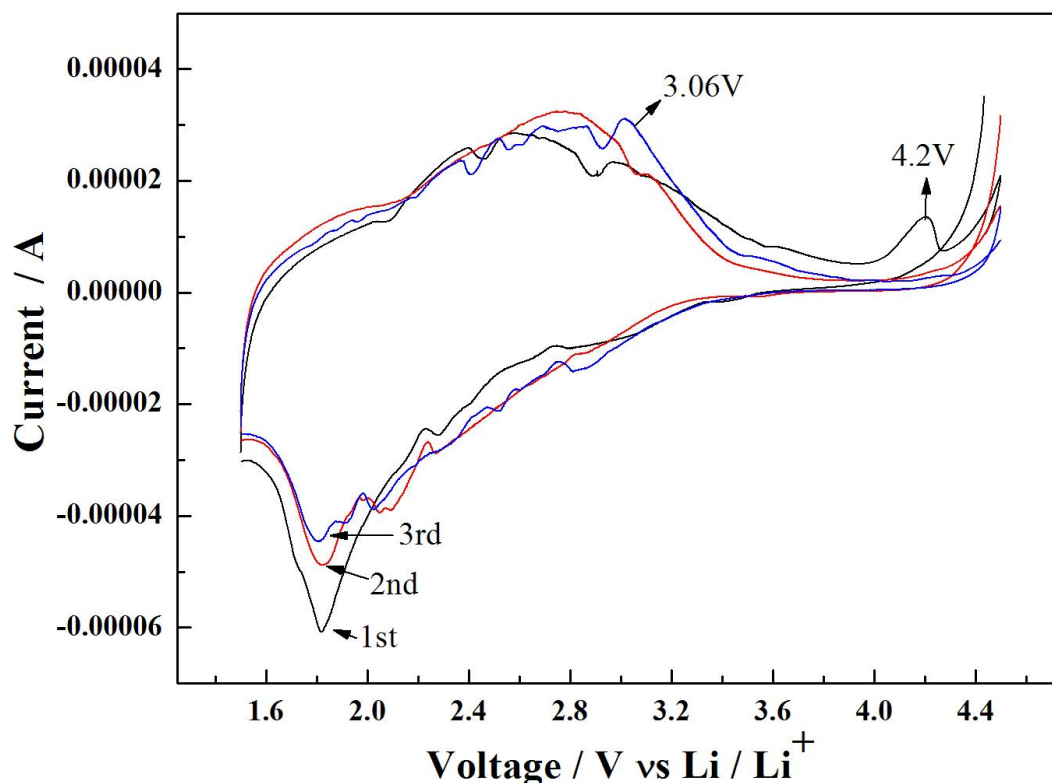

Figure 3. CV curves of the α-LiFeO$_2$ nanomaterials at the first three cycles

Figure 3 presents the CV curves at the first three cycles. From Figure 3, it is noted that an anodic peak at 4.2 V is observed in the first charge process, which agrees well with the

charge/discharge curve of Li/α-LiFeO$_2$ cell as shown in Figure 2d, and the 1.8 V peak abruptly decreases in the second cycle. In following cycles, an anodic peak at 4.2 V disappears, and new anodic and cathodic peaks appear at about 3 V (as marked in Figure 3). These results further demonstrate that the α-LiFeO$_2$ nanomaterials undergo a structural change during cycling.
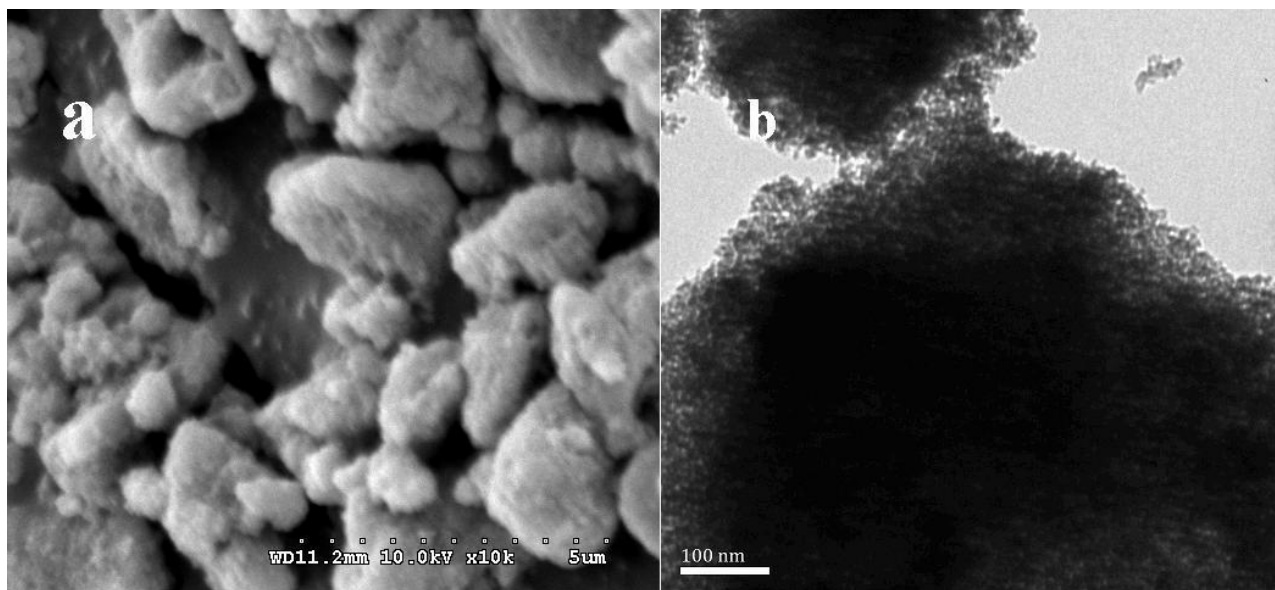

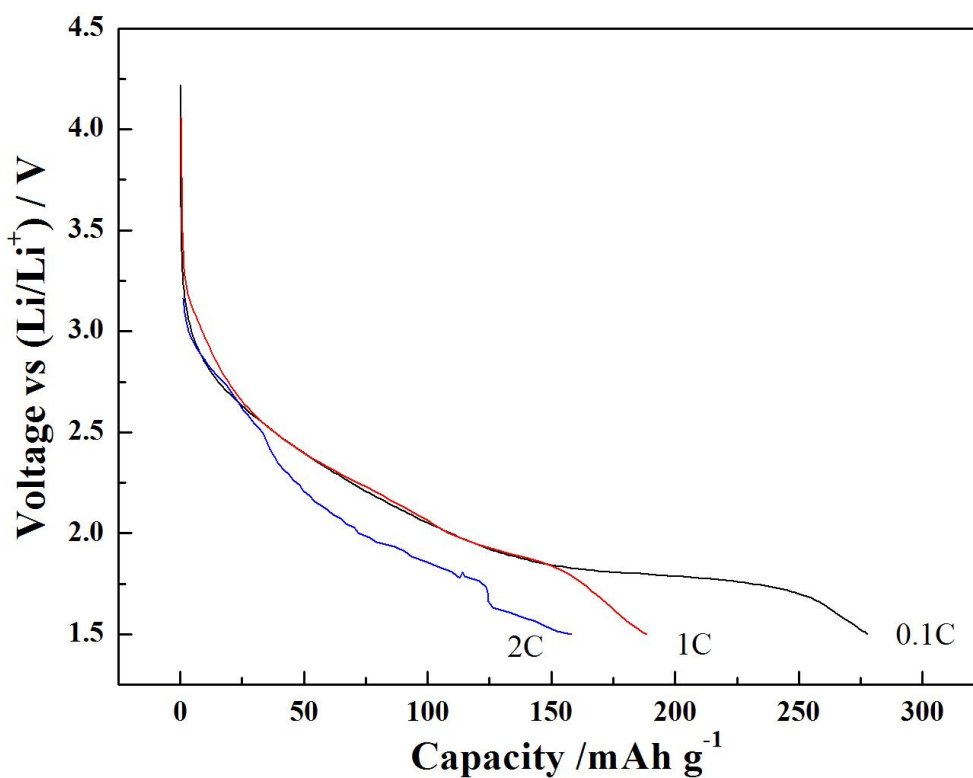**Figure 4.** SEM (a) and TEM (b) of the α-LiFeO$_2$ powder prepared at 250°C

Figure 5. The initial discharge curves of the α-LiFeO$_2$ nanomaterials at 0.1 C、1 C and 2 C

The morphology of the sample was investigated by SEM and TEM. Figure 4 shows SEM and TEM images of the α-LiFeO$_2$ particles synthesized at 250℃. The SEM pictures display that the α-LiFeO$_2$ powders are composed of very tiny nano particles. TEM investigations further reveal that the samples consist of tiny particles. From Figure 4b, it can be clearly seen that the resulting product has a rod-like morphology with average diameter of 2.5 nm and average length of 12.5 nm and a fairly narrow particle size distribution range, supporting the XRD results. The TEM pictures display the absence of agglomerates and ensure the high specific surface area of samples.

It should be noted that most of the previous reports were focused on very low rate charge/discharge current densities. Recently, more attentions have been paid to its rate capability. To evaluate its rate capability, the tests at different discharge current were conducted for the α-LiFeO$_2$ nanomaterials. Figure 5 shows the initial discharge curves of the α-LiFeO$_2$ nanomaterials at 0.1 C, 1 C and 2 C. From Figure 5, it can be seen that the initial discharge capacity is about 277.9, 188.4, and 158.2 mAh g^{-1} at 0.1 C, 1 C, and 2 C, respectively. In particular, at a discharge current as high as 2 C, the discharge capacity is still kept as high as 158.2 mAh g^{-1}, which is relatively high among all the nano-LiFeO$_2$ materials [8, 16]. The excellent rate performance could be attributed to the high phase purity, small and uniform particle size.
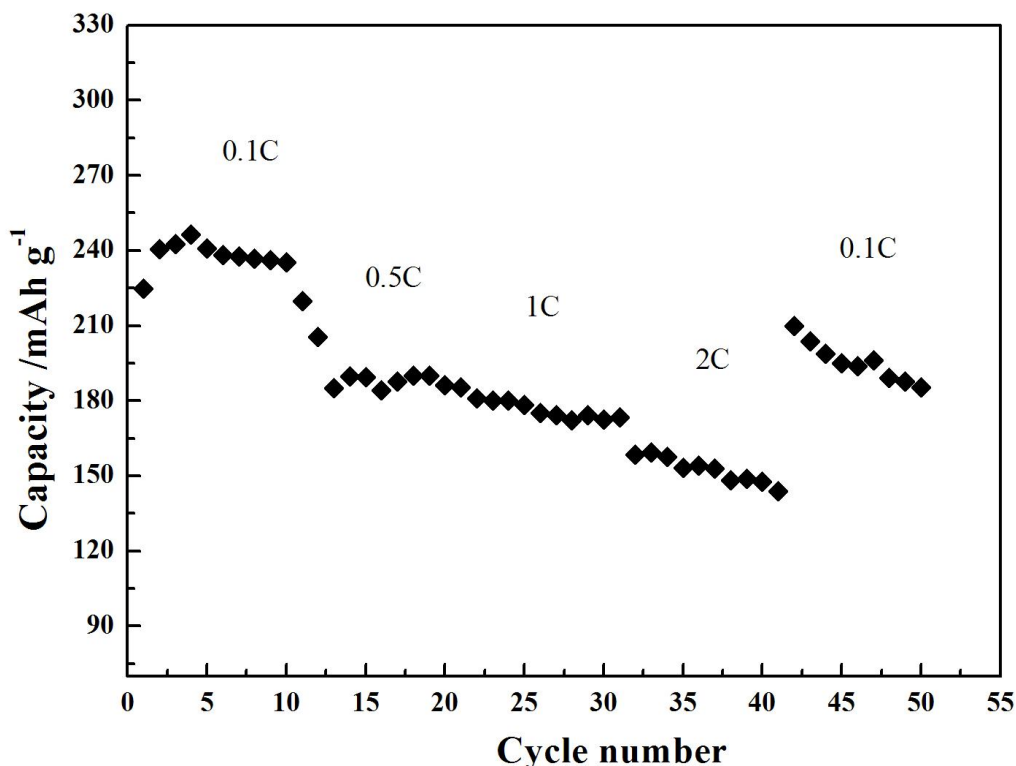

Figure 6. Rate capabilities of α-LiFeO$_2$ nanomaterials from 0.1C to 2 C for ten cycles.

The rate performance of the α-LiFeO$_2$ nanomaterials at 0.1 to 2 C was further investigated as shown in Figure 6. Figure 6 presents the rate capability of the α-LiFeO$_2$ nanomaterials from 0.1 to 2 C for ten cycles at each current rate, followed by a return to 0.1 C. At lower rates, the discharge

capacities at 0.1 C and 0.5 C are around 240 and 188 mAh g^{-1}, respectively. It can still retain 175 and 153 mAh g^{-1} at 1 C and 2 C, respectively. When the rate is decreased to 0.1 C after 40 cycles, the reversible capacity of the α-LiFeO$_2$ nanomaterial still reaches 200 mAh g^{-1}. These results indicate that the excellent rate performance and cycling stability can be obtained at each rate.
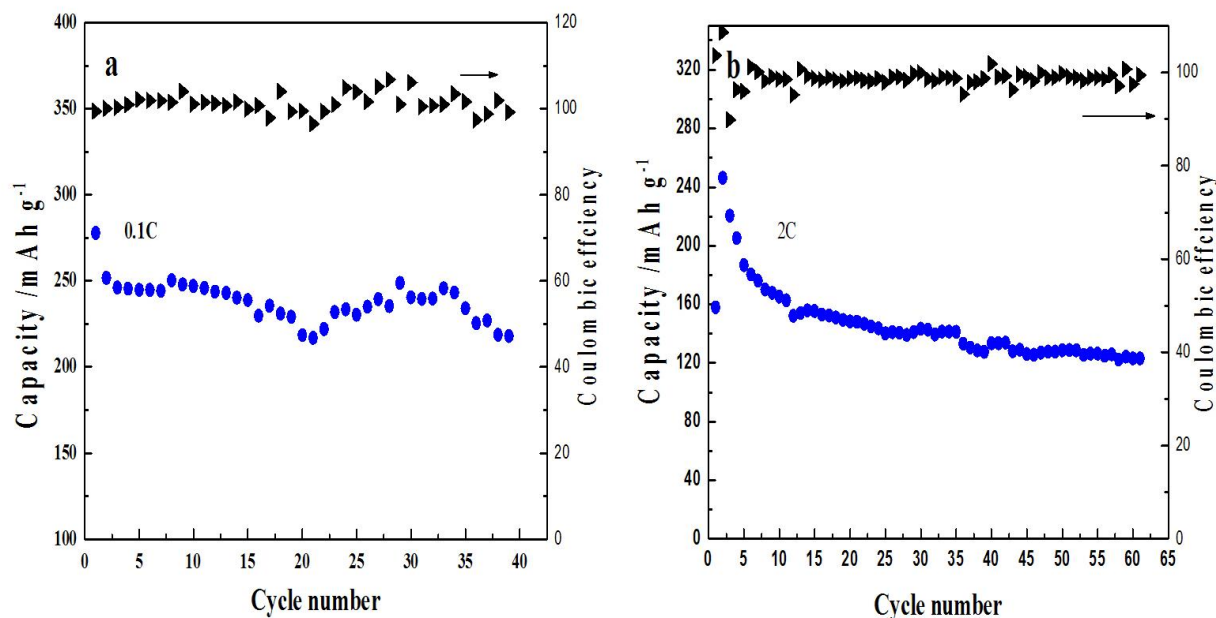

Figure 7. Cycling performances of the α-LiFeO$_2$ nanomaterials

Up to now, the cycling stability of the α-LiFeO$_2$ materials cannot meet the requirements. Figure 7a shows the cycling performance of the α-LiFeO$_2$ materials at a current drain of 0.1 C. It is noted that the discharge capacity has a weak decay at the beginning. The discharge capacity loss in the initial cycle's stems from the irreversible structure change and unusual Fe^{4+} ions generated during cycling [7]. After 40 charge–discharge cycles a reversible discharge capacity as high as 220 mAh g^{-1} can still be retained, and the coulombic efficiency (calculated from the discharge and charge capacities) approaches almost 100%. Meanwhile, Figure 7b clearly demonstrates that the nano-LiFeO$_2$ electrodes have excellent cycle ability and high coulombic efficiency even at 2 C, which can deliver a capacity of 123 mAh g^{-1} at 2 C after 60 cycles.

In summation, the electrochemical studies demonstrate that the α-LiFeO$_2$ materials exhibit a high reversible capacity, excellent cycling performance, and good rate capability.

4. CONCLUSION

The α-LiFeO$_2$ nanoparticles have been successfully prepared by low-temperature solid state method. The TEM results indicate the α-LiFeO$_2$ nanoparticles have a rod-like morphology with average diameter of 2.5 nm and average length of 12.5 nm, and a fairly narrow particle size

distribution range. The α-LiFeO₂ nanocomposite electrodes deliver a higher reversible capacity, rate performance and more stable cycle life. Especially, the high capacity of 158.3 mAh g^{-1} can be obtained at 2 C, which makes it a very promising cathode material for the lithium ion battery.

Reference

1. W. C. West, J. Soler, and B. V. Ratnakumar, *Journal of Power Sources* 204 (2012) 200.
2. Ting Li, Zhong X. Chen, Yu L. Cao, Xin P. Ai, Han and X. Yang, *Electrochimica Acta* 68 (2012) 202.
3. J. R. Croy, S.-H. Kang, M. Balasubramanian and M. M. Thackeray, *Electrochemistry Communications* 13(10) (2011) 1063.
4. Y. S. Lee, C. S. Yoon, Y. K. Sun, K. Kobayakawa and Y. Sato, *Electrochemistry Commuications* 4 (2002)727.
5. Md. Mokhlesur Rahman, J.Z. Wang, M.F. Hassan, S.L. Chou, Z.X. Chen and H.K. Liu, *Energy & Environmental Science* 4 (2011) 952–957.
6. X. Wang, L. Gao, F. Zhou, Z. Zhang, M. Ji, C. Tang, T. Shen, and H. Zheng, *Journal of Crystal Growth* 265 (2004)220.
7. Y. Sakurai, H. Arai and J. Yamaki, *Solid State Ionics* 113–115(1998) 29.
8. S. H. Wu and H. Y. Liu, *Journal of Power Sources* 174(2007) 789.
9. Y. Sakurai, H. Arai, S. Okada and J. Yamaki, *Journal of Power Sources* 68 (1997) 711.
10. T. Matsumura, R. Kanno, Y. Inaba, Y. Kawamoto and M. Takano, *Journal of Electrochemistry Society* 149 (2002) A1509.
11. Y. S. Lee, S. Sato, M. Tabuchi, C. S. Yoon, Y. K. Sun, K. Kobayakawa and Y. Sato, *Electrochemistry Communications* 5 (2003) 549.
12. Y. S. Lee, S. Sato, Y. K. Sun, K. Kobayakawa and Y. Sato, *Journal of Power Sources* 119–121 (2003)285.
13. L. Bordet-Le Guenne, P. Deniard, A. Lecerf, P. Biensan, C. Siret, L. Fournes and R. Brec, *Journal of Materials Chemistry* 9(1999) 1127.
14. R. Kanno, T. Shirane, Y. Inaba and Y. Kawamoto, *Journal of Power Sources* 68 (1997)145.
15. J. Morales and J. Santos-Pen, *Electrochemistry Communications* 9 (2007)2116.
16. Y. Ma, Y. Zhu, Y. Yu, T. Mei, Z. Xing, X. Zhang and Y. Qian, *International Journal of Electrochemical Science* 7 (2012)4657.
17. S. Uzunova, I. Uzunov, D. Kovacheva, A. Momchilov and B. Puresheva, *Journal of Apply Electrochemistry* 36 (2006) 1333.
18. Y. S. Lee, S. Sato, Y. K. Sun, K. Kobayakawa and Y. Sato, *Electrochemical Communications* 5 (2003)359.
19. J. Chen, L. Xu, W. Li and X. Gou, *Advance Materials* 17 (2005) 582.
20. C. Z. Wu, P. Yin, X. Zhu, C. OuYang and Y. Xie, *Journal of Physical Chemistry* B 110 (2006)17806.
21. C. Z. Wu, K. Yu, S. Zhang and Y. Xie, *Journal of Physical Chemistry* C 112 (2008) 11307.
22. S. Y. Zeng, K. B. Tang, T.W. Li, Z. H. Liang, D.Wang, Y. K.Wang and W. W. Zhou, *Journal of Physical Chemistry* C 111 (2007) 10217.

23. S. Y. Zeng, K. B. Tang, T.W. Li, Z. H. Liang, D.Wang, Y. X. Qi and W. W. Zhou, *Journal of Physical Chemistry* C 112 (2008)4836.
24. P. L. Taberna, S. Mitra, P. Poizot, P. Simon and J.M. Tarascon, *Nature Materials* 5(2006) 567.
25. Y. G. Guo, Y. S. Hu, W. Sigle and J. Maier, *Advanced Materials* 19 (2007) 2087.
26. M. Hirayama, H. Tomita, K. Kubota, H. Ido and R. Kanno, *Materials Research Bulletin* 47 (2012) 79–84.
27. A. Robert Armstrong, W. Tee Daniel, F.L. Mantia, P. Novák , and P. G. Bruce, *Journal of America Chemistry Society* 130 (2008) 3554.